Electronic properties of a cluster-based solid form of carbon: C_{28} hyperdiamond

Efthimios Kaxiras
Department of Physics, Harvard University, Cambridge, Massachusetts 02138
and Division of Applied Sciences, Harvard University, Cambridge, Massachusetts 02138

Linda M. Zeger
Department of Physics, Harvard University, Cambridge, Massachusetts 02138

A. Antonelli
Instituto de Fisica, Universidade Estadual de Campinas-Unicamp, Caixa Postal 6165, Campinas, Sao Paulo 13.081 Brazil

Yu-min Juan
Division of Applied Sciences, Harvard University, Cambridge, Massachusetts 02138
(Received 10 November 1993)

Using *ab initio* electronic structure calculations, we study a cluster-assembled form of carbon which is based on C_{28} units arranged in a diamond crystal (hyperdiamond). We investigate how the charge density and electronic spectrum of an isolated C_{28} unit is altered in the infinite lattice. We analyze the nature of electronic states near the Fermi level of both an isolated C_{28} cluster and its solid form. A tight binding model, with parameters fitted to reproduce energy eigenvalues calculated from first principles, provides insight on how the states of hyperdiamond are derived from those of C_{28}.

I. INTRODUCTION

The carbon structures which resemble graphitic cages (C_{60}, C_{70}, and their derivatives, known as fullerenes),[1] have aroused a great deal of interest for their role as molecules which can encapsulate atoms. Subsequent to the discovery that the C_{60} molecule and the larger fullerenes can serve as containers for atoms,[2] a smaller fullerene, C_{28}, was found to function similarly.[3] In addition to its ability to entrap an atom, the C_{60} molecule can also serve as a building block for a crystalline solid.[4] Likewise, one might consider whether a C_{28} cluster can serve not only as an atomic cage, but also as a unit from which a solid can be composed.[3,5]

In a C_{60} molecule all carbon atoms are threefold coordinated. The atoms are arranged in 12 pentagons and 20 hexagons, and produce a structure very close to graphite (the latter is composed exclusively of planar hexagons). Thus, the carbon atoms in C_{60} are bonded essentially through sp^2 hybrids, as in graphite. The spectrum of σ and π bonding states produced by the geometry and symmetry of C_{60} (icosahedral group I_h) accommodates all electrons in fully occupied states, producing a gap between the highest occupied molecular orbital (HOMO) and the lowest unoccupied molecular orbital (LUMO). This situation makes C_{60} quite stable and chemically unreactive. Hence, the intermolecular interactions in a solid composed of C_{60} units are rather weak, arising from van der Waals interactions.[6,7]

The structure for C_{28} (shown in Fig. 1), first proposed by Kroto,[8] obeys the T_d point group symmetry. All atoms are again threefold coordinated, and are arranged in 12 pentagons and 4 hexagons. Due to the larger ratio of the number of pentagons to hexagons in C_{28}, many orbitals of this cluster are of the sp^3 type rather than the graphitic sp^2 type found in C_{60}. In particular, the four atoms of an isolated C_{28} that form the apexes where triplets of pentagons meet (shown in black in Fig. 1) favor sp^3 bonding due to the nearly tetrahedral bond angles at these junctions. This sp^3 bonding produces "dangling

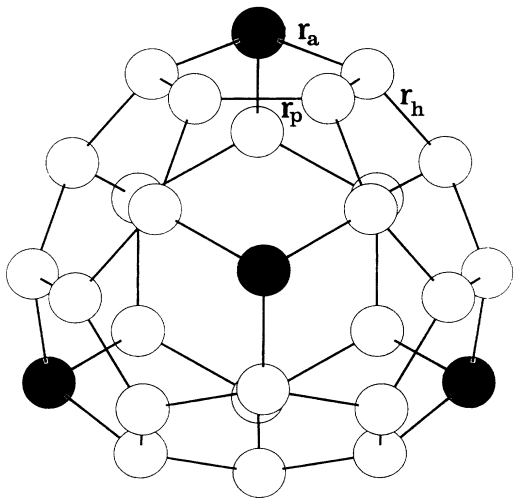

FIG. 1. The structure of the C_{28} cluster. The three atom types are (i) a black atom which forms the apex of three fivefold rings, (ii) a white atom which is part of a sixfold ring and is bonded to a black atom, and (iii) a different type of white atom which is part of a sixfold ring but is not bonded to a black atom. The resulting three different types of bonds are identified as r_a, r_p, and r_h.

bonds" (orbitals that cannot effectively bond with other nearest neighbor states), and results in a partially occupied HOMO which renders an isolated C_{28} cluster unstable, in contrast to a C_{60} molecule. The C_{28} cluster can be stabilized when it is produced in the presence of U, Ti, Zr, or Hf atoms which become encapsulated in the cage.[3,9,10] Alternatively, it is conceivable that C_{28} units could be stabilized by saturating their dangling bonds externally through covalent bonding, either with other atoms such as H,[3,11–13] or, as suggested recently,[3,5] through bonds between C_{28} units themselves. The black apex atoms of C_{28}, on which the dangling bonds are centered, lie on the vertices of a tetrahedron, which makes this cluster behave as a tetravalent superatom. Guided by the tetrahedral arrangement of individual carbon atoms found in diamond, one might expect that a diamond lattice constructed from C_{28} units, as shown in Fig. 2, would be a reasonable candidate for a solid based on this small fullerene[3,5]. The bonding between C_{28} units in such a solid would be covalent, due to strong interactions among the half filled tetrahedral dangling bonds. This strong bonding is quite different from the comparatively weak van der Waals forces responsible for bonding C_{60} units together in its solid form. The structural properties of an arrangement of the C_{28} units in the diamond lattice [called hyperdiamond $(C_{28})_2$] have been studied by Bylander and Kleinman[5]. In this work we concentrate on the electronic properties of this hypothetical solid.

The rest of this paper is organized as follows. Section II describes briefly the first principles methodology employed in this work. Section III discusses the structure and properties of the isolated cluster. Section IV describes the structural features of the hypothetical solid, hyperdiamond. Section V gives a detailed analysis of its electronic properties. Finally, Section VI draws some conclusions regarding the possibility of forming this type of solid and its utility.

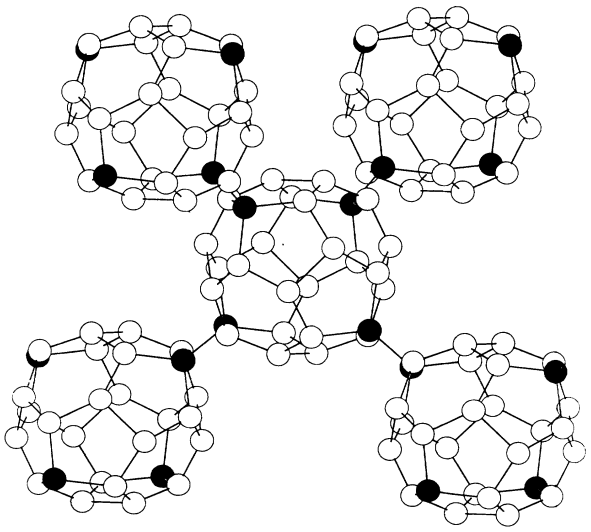

FIG. 2. Structure of the hyperdiamond lattice. The C_{28} clusters are bonded together at the black atoms.

II. METHODOLOGY

We use *ab initio* calculations to obtain total energies and electronic densities, as well as single particle electronic states and eigenvalues. The calculations are performed within the framework of density functional theory using the local density approximation (LDA) (Ref. 14) to treat the exchange and correlation contributions to the total energy.[15] The ionic potential, including the screening from core electrons, is modeled by a nonlocal norm conserving pseudopotential,[16] which is rather "soft" (it produces convergence with relatively few Fourier components, as established by Kaxiras and Pandey,[17] from studies of the energetics of local distortions in graphite). The s and p components of the ionic potential are included in the calculation, and the Kleinman-Bylander scheme[18] is employed to make the potential separable in Fourier space. The electronic wave functions are expanded in a plane wave basis set with an energy cutoff up to 28 Ry. The Γ point (the center of the irreducible Brillouin zone) is used for sampling the charge density for the total energy calculations.

We use the molecular dynamics method of Car and Parrinello[19] to solve the Kohn-Sham equations and compute the ground state energy and optimal lattice constant of hyperdiamond. The electronic wave functions are evolved to self-consistency at several values of the lattice constant through a steepest descent algorithm. Once the equilibrium lattice constant is found, the single particle eigenstates and eigenvalues are calculated at additional reciprocal space points with a smaller plane wave energy cutoff (18 Ry).

We have performed calculations for isolated clusters in a supercell geometry, as well as for the hyperdiamond solid. In the latter case we have considered three different geometries of the C_{28} unit. These geometries were taken from: (a) restricted Hartree-Fock calculations for an isolated C_{28} cluster, reported by Guo *et al.*;[3] (b) LDA calculations, including full relaxation for the isolated cluster within the tetrahedral symmetry group, reported by Jackson, Kaxiras, and Pederson;[13] and (c) LDA calculations for the hydrogenated cluster including full relaxation within the tetrahedral symmetry group, also from Jackson, Kaxiras, and Pederson.[13] The crystal structure based on the LDA geometry (c) gives the lowest energy for the solid in our calculations. We use the geometry (b) for the isolated cluster calculation.

III. STRUCTURE AND PROPERTIES OF THE ISOLATED CLUSTER

The structure of an isolated C_{28}, shown in Fig. 1, consists of four sixfold rings (distorted hexagons) and twelve fivefold rings (distorted pentagons). Unlike the twelve fivefold rings in C_{60}, which do not share vertices or edges, the fivefold rings in C_{28} are adjacent to one another. These rings are grouped in triplets sharing a common atom (shown in black in Fig. 1), with each fivefold ring having three common edges with other fivefold

rings, two edges with fivefold rings of the same triplet and one edge with a fivefold ring belonging to another triplet. There are three distinct atom types in a C_{28} cluster: the black atom, which forms the junction of three fivefold rings, a second type of atom which has one bond to a black atom, and a third type of atom which has no bonds to a black atom. Atoms of the second and third types are shown in white in Fig. 1. The 24 white atoms form four sixfold rings, the centers of which are diametrically across from the black atoms. The three distinct atom types produce three distinct bond types in C_{28}. In our isolated cluster calculations we choose the bond lengths according to the optimized geometry found by Jackson, Kaxiras, and Pederson:[13] r_a=1.446 Å between a black and a white atom, r_p=1.510 Å between two white atoms that link two sixfold rings, and r_h=1.428 Å between two white atoms within a sixfold ring (see Fig. 1).

In Fig. 3(a) we show the total valence charge density in a plane that contains two black atoms and the center of the cage (which is also the geometrical center of

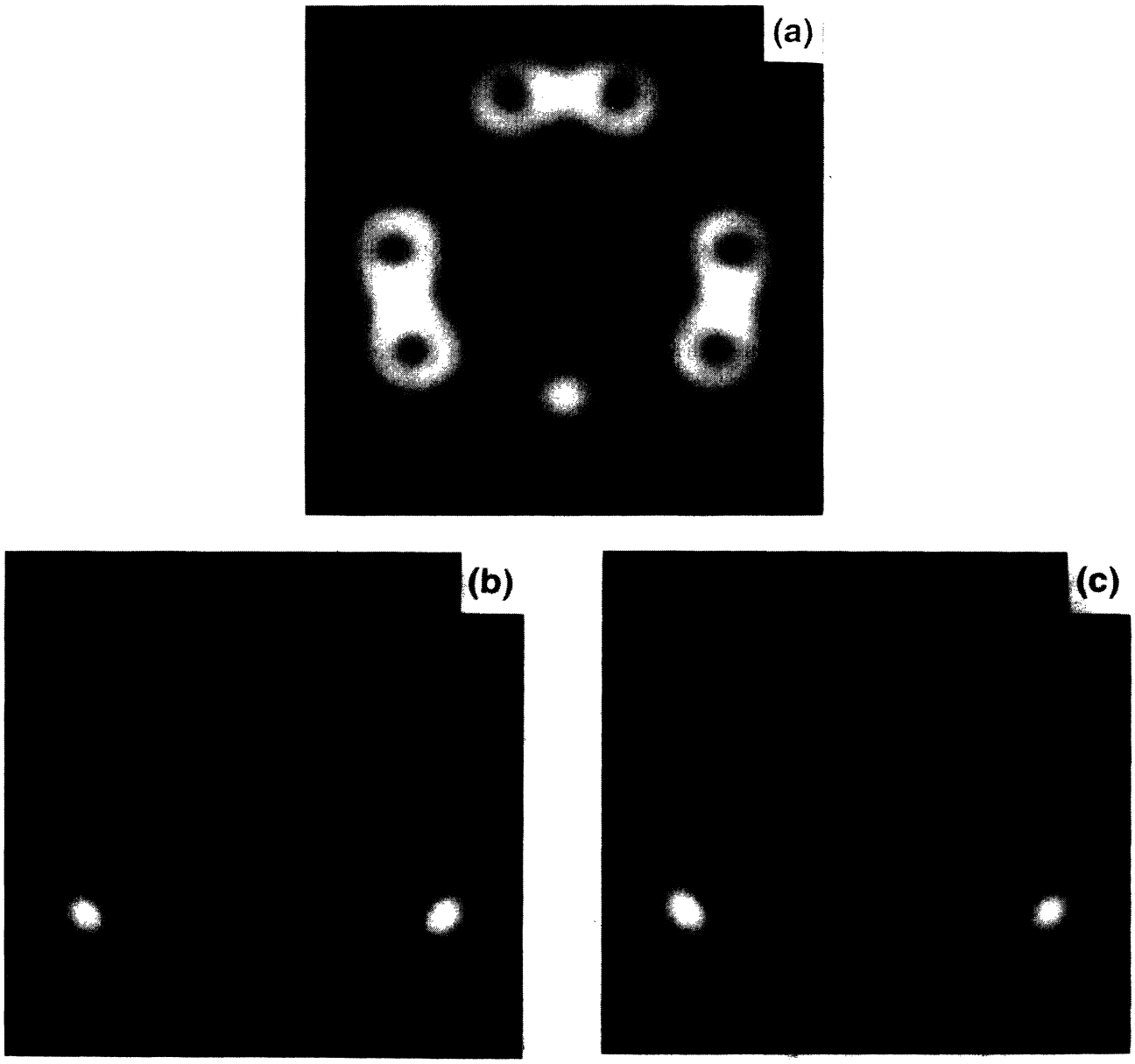

FIG. 3. (a) The total valence charge density on a cross section of the C_{28} cluster. The scale of electron density is represented by the brightness (the highest electron density is white). Each nearly vertical bond at the lower left and lower right hand sides of the figure is between one black atom and one white atom. Two different views of a bond between two white atoms that are not bonded to black atoms are shown at the top and bottom center of the figure. The upper bond is parallel to the plane of the figure and its entire length is shown, while the lower bond is perpendicular to the figure and a cross section at its midpoint is shown. Wave-function magnitude of the states near the Fermi level for (b) the triplet state t_2 (HOMO) and, (c) the singlet state a_1 (LUMO).

the tetrahedron formed by the black atoms). This plane contains two bonds of length r_a (the two nearly vertical bonds at the lower left and lower right sides of the figure) and one bond of length r_p (horizontal bond on the upper part of the figure), while it bisects another bond that has length r_p (circular cross section at the bottom center of the figure). All subsequent figures displaying charge densities and wave-function magnitudes are on the same plane. This plane was identified by Dunlap, Häberlen, and Rösch[9] as a covenient choice for discussing wave functions and charge densities because it contains all the symmetry unrelated atoms in the cluster. From Fig. 3(a) it is seen clearly that the bonds have covalent character, with most of the valence charge density concentrated near the midpoints of the interatomic distances. Comparing the cross sections from the two different bond types shown, we note that the r_a bond corresponds to a slightly higher charge density than the r_p bond. Although both r_a and r_p bonds form the edges of fivefold rings, they differ in that the former bond serves as a link between a sixfold ring and a fivefold ring, while the latter bond links two sixfold rings (see Fig. 1). The greater charge density found on the bond which links a fivefold ring to a sixfold ring can be explained by the observation[3] that the greatest strain in the fullerene structures is located at the vertices of fivefold rings, particularly where several of them are adjacent.[20] The r_a bond is also shorter (i.e., stronger) than the r_p bond, which is consistent with the charge distribution shown in Fig. 3(a).

Examination of the nature of states near the Fermi level reveals the locations of the cluster's chemically active sites. It is no surprise that the regions of greatest strain in the C_{28} structure, where triplets of fivefold rings meet at black atoms, are also the sites of highest chemical reactivity. The wave-function magnitude $|\phi^{(n)}(\vec{r})|^2$ of the HOMO and LUMO states is shown in Figs. 3(b) and 3(c), respectively. The states near the Fermi level consist of a triplet HOMO (t_2), and a singlet LUMO (a_1). The eigenstates of C_{28} have degeneracies of 1, 2, and 3, which are the ones allowed by the dimensions of the irreducible representations of the T_d point group. The wave-function magnitudes of the t_2 and a_1 states [Figs. 3(b) and 3(c), respectively] are most heavily concentrated at the black atoms. The HOMO wave function is essentially identical to that described by Rösch, Häberlen, and Dunlap[21] for the Ce@C_{28} complex, when the endohedral component is subtracted out. The orbitals of these states are oriented so that they point predominantly outward from the cluster. In fact, little wave-function magnitude from these states lies between a black atom and its neighboring white atoms. Thus, the states near the Fermi level can be identified as dangling bond orbitals located at the four black atoms. The t_2 state can accommodate six electrons (triply degenerate) and the a_1 state two electrons (singly degenerate), when electron spin is taken into account. Because only four electrons are occupying these states and the energy of the a_1 state is slightly higher than that of the t_2 state, the t_2 state is partially occupied (2/3 filled), while the a_1 state is vacant. This situation makes the cluster unstable as a result of the presence of partially filled orbitals centered at the four black atoms.

IV. STRUCTURE OF THE SOLID

Since C_{28} has tetrahedral symmetry and its eigenstates near the Fermi level are hybrids pointing towards the vertices of a tetrahedron, this molecule is analogous to tetravalent atoms, which typically form four sp^3 hybrids. This similarity suggests that the diamond lattice is a natural candidate for a solid built from C_{28} units.[3,5] Although other structures composed of these units may exist in solid form, in this work we focus on the diamond

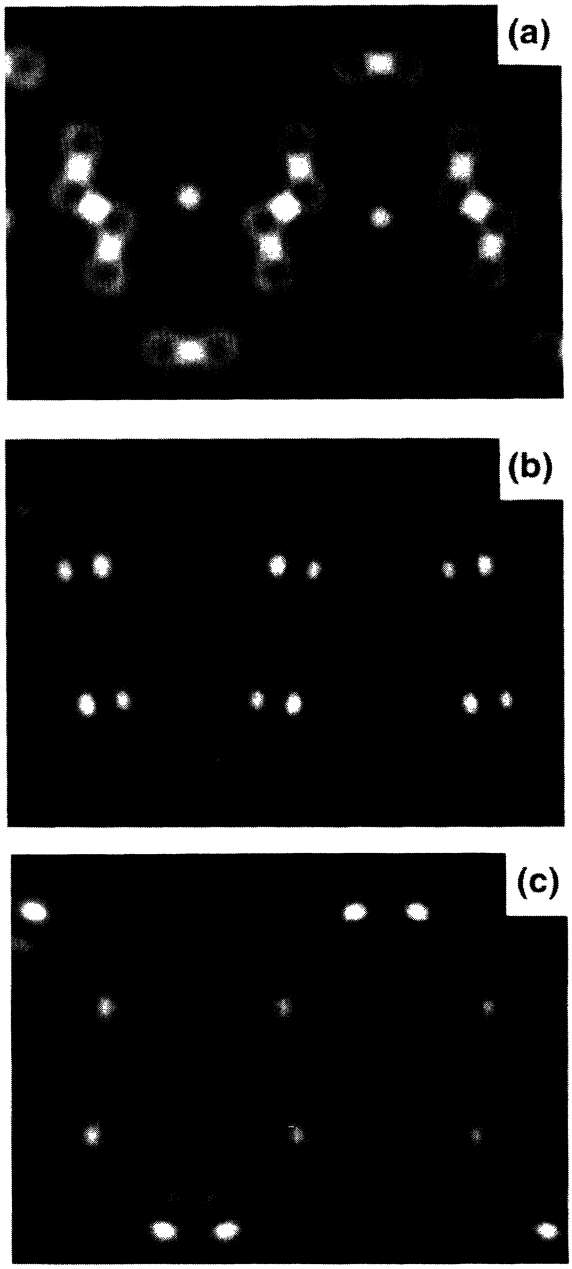

FIG. 4. (a) Valence charge density of hyperdiamond on the (110) plane. The only significant change from the charge density of an isolated C_{28} cluster is that intercluster bonds are formed at the tetrahedral apex atoms. Wave-function magnitude at Γ of hyperdiamond on the (110) plane for (b) the highest VBM state and (c) the lowest CBM state.

lattice as the simplest choice of a solid composed of C_{28} units. The structure of this lattice, called hyperdiamond, is shown in Fig. 2. Since the dangling bond orbitals are located on the black atoms, we construct the diamond lattice so that bonds between clusters occur at these locations. Our total energy calculations for the solid yield a lattice constant equal to 16.4 Å, which corresponds to a minimum distance between two clusters (the bond length between two black atoms on adjacent C_{28} units) of 1.54 Å. This value lies in the range expected for singly bonded carbon atoms with sp^3 bonding (for comparison, the bond length between two C atoms in diamond is also 1.54 Å). These results are close (within few percent) to the values obtained in the more thorough study of structural features by Bylander and Kleinman, which used 40 Ry cutoff for the plane-wave basis and 64 points in the Brillouin zone.[5] For example, the bond between black atoms on adjacent clusters found by Bylander and Kleinman is 1.53 Å. Thus, the largest difference in the geometries used in the two calculations is a distortion of the cage itself.

The total charge density of hyperdiamond in the (110) plane, shown in Fig. 4(a), remains practically unaltered from that of the isolated cluster seen in Fig. 3(a). There is only one significant change, namely that a bond is formed between two adjacent clusters at the black atoms. Thus, each cluster behaves almost like an autonomous entity, interacting strongly with its neighbors at the four reactive sites (black atoms), while preserving most of its internal electronic structure. Another confirmation of this property can be seen from the calculated density of states (DOS) shown in Fig. 5. Although there is some broadening of levels due to dispersion from the interaction between clusters, essentially all the features in the DOS of hyperdiamond can be traced to features in the DOS of the isolated C_{28} cluster.

V. ELECTRONIC PROPERTIES OF THE SOLID $(C_{28})_2$

In the preceding section we noted that a C_{28} cluster can be treated as a superatom, because it maintains most of its intrinsic characteristics when placed in an infinite crystalline lattice. In this section we use this perspective to gain insight into the band structure of hyperdiamond near the Fermi level. We first note that the dangling bond states of an isolated C_{28}, which are the states closest to the Fermi level, are shifted in energy when the clusters are brought together to form hyperdiamond. This change is a result of the strong interaction between sp^3 orbitals of neighboring clusters at the tetrahedral apex atoms; hence, the bonding (antibonding) states formed from combinations of orbitals centered on black atoms end up far below (above) the Fermi level of the solid. An important consequence of this splitting of bonding and antibonding combinations is the creation of a large gap in the band structure of hyperdiamond (see Figs. 5 and 6). Our results give a direct gap at Γ equal to 1.61 eV. Taking into account the well known tendency of LDA to underestimate the gaps of semiconductors by approximately 50%,[22] we expect that in the real solid, if it can be produced, this gap will be close to 3 eV. The minimum gap is indirect; it is between a threefold degenerate occupied state at Γ and a twofold degenerate unoccupied state near the L edge of the Brillouin zone.

The states of hyperdiamond that are most relevant to the properties of the solid are the ones just above and just below the Fermi level, by analogy to the solid form of C_{60}. In the latter case, the properties of the solid were deduced by using detailed first principles calculations,[23] as well as simple models that capture the essential physics (see, for example, the tight binding analysis of Manousakis[24]). In this work we analyze the states of hyperdiamond near the Fermi level from both perspectives. The states near the Fermi level are derived from combinations of different orbitals on the C_{28} clusters. The resulting bands can

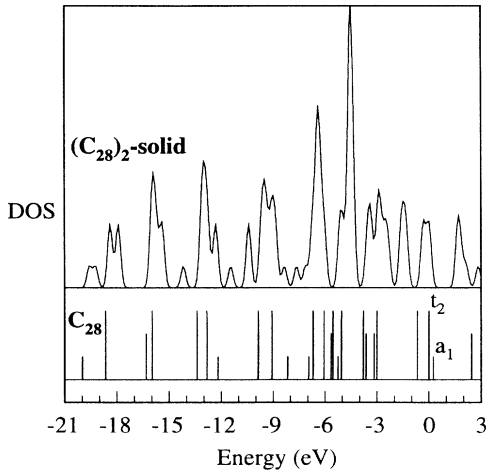

FIG. 5. Density of states of hyperdiamond (upper portion) and an isolated C_{28} cluster (lower portion). The density of states for hyperdiamond is obtained from the states at the Γ, X, and L points, with proper weights. The zero of energy is that of the HOMO of C_{28}.

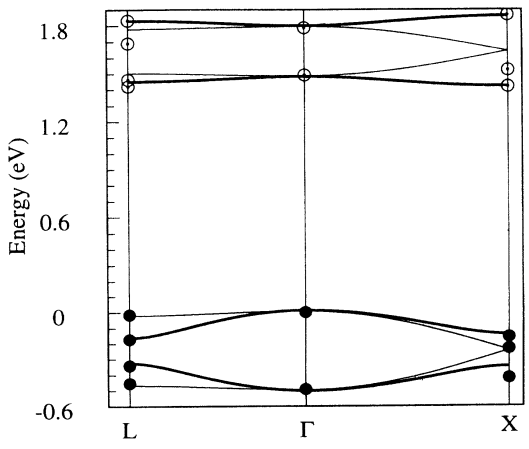

FIG. 6. Band structure of hyperdiamond calculated from a tight-binding model (solid lines) with parameters fitted to approximately reproduce the LDA eigenvalues (open and filled dots for states above and below the Fermi level, respectively) at the Brillouin zone center and edges.

be described within a simple tight-binding (TB) picture by assigning two triplets of states of p-type character to each cluster.[25] Six states, a p-type triplet from each cluster, are combined to produce the crystal bands below the Fermi level, while the remaining p-type states from each cluster combine to form the bands above the Fermi level. We refer to the first six states below the Fermi level collectively as the valence band maximum (VBM) bands, since their band width is small (about 0.5 eV) compared to the total band width (about 21 eV, see Fig. 5). For the same reason, we refer to the first six states above the Fermi level collectively as the conduction band minimum (CBM) bands. In this TB picture the VBM bands are given by

$$\epsilon_1^{\Gamma X}(k) = \epsilon_p \pm \sqrt{8} \mid V_1 \mid [1+\cos(\pi k)]^{\frac{1}{2}}, \tag{1}$$

$$\epsilon_2^{\Gamma X}(k) = \epsilon_p \pm \sqrt{8}\left[V_1^2 + V_2^2 + (V_1^2 - V_2^2)\cos(\pi k)\right]^{\frac{1}{2}}, \tag{2}$$

in the ΓX direction. Here ϵ_p, V_1, and V_2 are adjustable parameters of the TB model. Each of the two ϵ_1 states is singly degenerate, whereas each ϵ_2 state is twofold degenerate. The VBM bands in the ΓL direction are given by

$$\epsilon_1^{\Gamma L}(k) = \epsilon_p \pm \Big[(V_1+2V_2)^2 + (3V_1-2V_2)^2 + 2(V_1+2V_2)(3V_1-2V_2)\cos(\pi k)\Big]^{\frac{1}{2}}, \tag{3}$$

$$\epsilon_2^{\Gamma L}(k) = \epsilon_p \pm \Big[(V_1-V_2)^2 + (3V_1+V_2)^2 + 2(V_1-V_2)(3V_1+V_2)\cos(\pi k)\Big]^{\frac{1}{2}}. \tag{4}$$

In Eqs. (1)–(4) the wave number k takes values in the interval $[0,1]$. A similar set of equations with a different set of adjustable parameters describes the CBM bands, which are built from the other set of p-type triplets. The adjustable parameters, V_1 and V_2 are expressed in terms of the usual orthogonal tight-binding Hamiltonian parameters $V_{pp\sigma}$ and $V_{pp\pi}$ (see, for example, Harrison[26]) in the following way:

$$V_1 = \frac{1}{3}(V_{pp\sigma} + 2V_{pp\pi}), \tag{5}$$

$$V_2 = \frac{1}{3}(V_{pp\sigma} - V_{pp\pi}). \tag{6}$$

The band structure of hyperdiamond calculated from this TB model is shown in Fig. 6. The TB parameters were obtained so as to approximately reproduce the LDA eigenvalues at the Brillouin zone center and at the L and X boundaries (filled dots for the VBM and empty dots for the CBM). As seen from Fig. 6, this simple TB model with only three adjustable parameters for each set of states is sufficient to account for the basic features of the LDA calculations. The presence of an indirect minimum band gap is evident in this figure. The lowest unoccupied state throughout the Brillouin zone is a twofold degenerate state. At the Γ point, this doublet appears to be part of a threefold degenerate state, within the accuracy of our calculations. We note that since there is only one bond connecting any two clusters and most of the states are not altered much by the *intercluster* interactions, the individual energy bands show very little dispersion (of order 0.1 eV), compared to that found in the diamond lattice (of order 10 eV). In particular, the lowest doubly degenerate unoccupied state disperses downward by 0.07 eV both in the ΓL and in the ΓX directions. All of these features are consistent, within the accuracy of our calculations, with the first principles results of Bylander and Kleinman.[5] The values of the TB parameters that give these fits are $V_{pp\sigma} = 0.0183, V_{pp\pi} = 0.0873$ for the VBM states and $V_{pp\sigma} = 0.1454, V_{pp\pi} = -0.0151$ for the CBM states (in eV). These values are more than an order of magnitude smaller than the hopping matrix elements obtained by Manousakis (~ 2.5 eV) to represent the states *within* a C_{60} cluster.[24] This is due to the fact that the present TB model describes *intercluster* interactions other than the covalent bonding between neighboring C_{28} units. These interactions are much weaker than typical *intracluster* interactions, which are comparable to bonding in graphite.

In order to gain insight into the nature of the VBM and CBM states, we studied their wave functions as given by our first principles calculations. The wave-function magnitudes $\mid \phi_{\vec{k}}^{(n)}(\vec{r}) \mid^2$ of the highest VBM state and the lowest CBM state at $\vec{k} = 0$ are displayed in Figs. 4(b) and 4(c), respectively. The wave-function magnitude in Fig. 4(b) is seen to lie primarily on the 12 white atoms that are bonded to black atoms. Fig. 4(b) gives the impression that this state is composed of noninteracting dangling bonds on these 12 white atoms. However, the large wave function magnitude around these atoms will also contribute to π bonding between these atoms and their neighbors that form the edges of the sixfold rings (the bonds of sixfold rings are not visible on the plane of this figure to make this π bonding evident). Furthermore, in the crystal wave function shown in Fig. 4(b), orbitals on equivalent atoms of neighboring clusters are nearly parallel, suggesting that this triply degenerate VBM state has π-type character. The wave-function magnitude depicted in Fig. 4(c) is a linear combination of orbitals at the other 12 white atoms which are *not* bonded to black atoms. From this figure, π bonding between these white atoms can be seen directly.

Further insight into the nature of the VBM and CBM bands is obtained from the magnitude of the relevant TB parameters: The ratio $\mid V_{pp\pi}/V_{pp\sigma} \mid$ for the VBM bands is equal to 6.33, while the same ratio for the CBM bands equals 0.11. Thus, the VBM states are composed primarily of π-type bonding combinations of p-type states associated with the individual C_{28} clusters, consistent with

the parallel orientation of orbitals on neighboring clusters shown in Fig. 4(b). The small ratio of $|V_{pp\pi}/V_{pp\sigma}|$ for the CBM states is suggestive of σ-type interactions, although this is not immediately evident from the wavefunction magnitude of these states at Γ. Finally, we note that the band structure of the solid is affected very little by the geometry of the cluster. For all three geometries that we have considered (see Sec. II), all the band structure features described above were the same, except for small overall shifts in energy.

VI. SUMMARY AND CONCLUSIONS

In summary, we have performed first principles total energy calculations to study the structural and electronic properties of hyperdiamond, a hypothetical solid formed by joining C_{28} units in an infinite lattice. A band gap is created when the reactive sites (black atoms) of the individual C_{28} units form covalent bonds with equivalent atoms in neighboring clusters. The basic features of the energy bands of hyperdiamond near the Fermi level are described by a simple tight-binding model. This model and the wave functions of the bands reveal that the states just above and just below the Fermi level are linear combinations of orbitals at the 24 white atoms of individual C_{28} clusters, which do not participate in the bonding of the solid. If this solid can be realized experimentally, the character of these states might prove important in understanding transport properties and other collective effects, as is the case for the alkali doped C_{60} crystals.[23,24]

We conclude by briefly discussing the possibility of forming the $(C_{28})_2$ hyperdiamond lattice and related solids. In order to form the perfect $(C_{28})_2$ crystal, each cluster must be precisely oriented. Even small deviations in the relative orientation of clusters will destroy the lattice periodicity. However, since a C_{28} cluster is a large object on the atomic scale, we expect that it will be difficult to orient these units properly in a solid. The unavoidable local defects suggest that a tetrahedrally bonded amorphous network of C_{28} clusters (which we shall call a-C_{28}) may be easier to obtain experimentally than the hyperdiamond crystal. The a-C_{28} phase will be porous with voids that are large on the atomic scale, and thus may serve as a good storage medium. If most of the dangling bonds at the apex atoms of C_{28} units are saturated through intercluster bonding in a-C_{28}, this material will also be a good insulator, in contrast to the known form of amorphous carbon, a-C. Both a-C_{28} and a-C consist primarily of threefold coordinated atoms,[27] with a small percentage of tetrahedral coordination. However, they are structurally very different: a-C_{28} would comprise a network of C_{28} units connected at the tetrahedral apex atoms, while a-C is believed to consist of planar threefold coordinated atoms, with occasional fourfold coordination altering the orientation of the planes.[27] We expect that a-C_{28} will have essentially the same electronic structure as hyperdiamond, with the bands broadened by disorder. The dispersion of states near the Fermi level of hyperdiamond is small compared to the band gap. This suggests that states near the Fermi level of a-C_{28} will exhibit only small band tails, thus preserving a sizable band gap, comparable to that of $(C_{28})_2$. The expected nonvanishing of the gap in a-C_{28} is the result of the favorable local arrangement of the threefold coordinated atoms, which allows extensive π bonding in the sixfold rings on individual cluster units. Another form of amorphous carbon expected to be insulating, the diamondlike amorphous carbon,[28] is actually metastable and is therefore unlikely to be found experimentally. Thus the a-C_{28} phase may prove to be a new and useful solid form of carbon, distinct from existing amorphous forms and easier to obtain than the crystalline form.

ACKNOWLEDGMENTS

The first-principles calculations were carried out at the Pittsburgh Supercomputer Center's Cray Y-MP and C90 supercomputers. This work was supported in part by Office of Naval Research Contract No. N00014-92-J-1138. A. Antonelli gratefully acknowledges the hospitality of the Physics Department and the Division of Applied Sciences of Harvard University, where this work was carried out.

[1] H.W. Kroto *et al.*, Nature **318**, 162 (1985).
[2] R.F. Curl and R.E. Smalley, Science **242**, 1017 (1988); Y. Chai *et al.*, J. Phys. Chem. **95**, 7564 (1991); J.H. Weaver *et al.*, Chem. Phys. Lett. **190**, 460 (1991).
[3] T. Guo *et al.*, Science **257**, 1661 (1992).
[4] S. Liu, Y. Lu, M. Kappes, and J. Ibers, Science **254**, 408 (1991).
[5] D. Bylander and L. Kleinman, Phys. Rev. B **47**, 10 967 (1993).
[6] Y. Wang, D. Tomanek, and G.F. Bertsch, Phys. Rev. B **44**, 6562 (1991).
[7] M.R. Pederson, K.A. Jackson, and L.L. Boyer, Phys. Rev. B **45**, 6919 (1992).
[8] H. Kroto, Nature **329**, 529 (1987).
[9] B. I. Dunlap, O. Häberlen, and N. Rösch, J. Phys. Chem. **96**, 9095 (1992).
[10] M. Pederson and N. Laouini, Phys. Rev. B **48**, 2733 (1993).
[11] O.D. Häberlen, N. Rösch, and B. I. Dunlap, Chem. Phys. Lett. **200**, 418 (1992).
[12] T. Guo, R. E. Smalley, and G. E. Scuseria, J. Chem. Phys. **99**, 352 (1993).
[13] K. Jackson, E. Kaxiras, and M. Pederson, Phys. Rev. B **48**, 17 556 (1993).
[14] P. Hohenberg and W. Kohn, Phys. Rev. **136**, B864 (1964); W. Kohn and L. Sham, Phys. Rev. **140**, A1133 (1965).
[15] We use the expressions for the exchange-correlation functionals proposed by J. Perdew and A. Zunger, Phys. Rev. B **23**, 5048 (1984).
[16] G. Bachelet, H. Greenside, G. Barraff, and M. Schlüter, Phys. Rev. **24**, 4745 (1981).
[17] E. Kaxiras and K.C. Pandey, Phys. Rev. Lett. **61**, 2693 (1988).

[18] L. Kleinman and D.M. Bylander, Phys. Rev. Lett. **48**, 1425 (1982).
[19] R. Car and M. Parrinello, Phys. Rev. Lett. **55**, 2471 (1985).
[20] T. G. Schmalz, W. A. Seitz, D. J. Klein, and G. E. Hite, J. Am. Chem. Soc. **110**, 1113 (1988).
[21] N. Rösch, O. D. Häberlen, and B. I. Dunlap, Angew. Chem. Int. Ed. Engl. **32**, 108 (1993).
[22] J. Perdew and M. Levy, Phys. Rev. Lett. **51**, 1884 (1983); L. Sham and M. Schlüter, *ibid.* **51**, 1888 (1983); M. Hybertsen and S. Louie, *ibid.* **55**, 1418 (1985); R. Godby, M. Schlüter, and L. Sham, *ibid.* **56**, 2415 (1986).
[23] S.C. Erwin, M.R. Pederson, and W.E. Pickett, Phys. Rev. B **41**, 10437 (1990); S. Saito and A. Oshiyama, Phys. Rev. Lett. **66**, 2637 (1991); S.C. Erwin and W.E. Pickett, Science **254**, 842 (1991); S.C. Erwin and M.R. Pederson, Phys. Rev. Lett. **67**, 1610 (1991); N. Trouiller and J.L. Martins, Phys. Rev. B **46**, 1754 (1992); J.L. Martins and N. Trouiller, *ibid.* **46**, 1766 (1992); W. Andreoni, F. Gygi, and M. Parinello, Phys. Rev. Lett **68**, 823 (1992).
[24] E. Manousakis, Phys. Rev. B **44**, 10991 (1991).
[25] We refer to the states associated with the C_{28} clusters which participate in the formation of bands as "*p* type," in order to distinguish them from orbitals associated with individual C atoms. Similarly, we call intercluster bonding that results from parallel orientations of these states "π-type" bonding, to distinguish it from π bonding between atomic orbitals on individual C atoms.
[26] W.A. Harrison, *Electronic Structure and the Properties of Solids* (Freeman, San Francisco, 1980).
[27] D. Beeman, J. Silverman, R. Lynds, and M.R. Anderson, Phys. Rev. B **30**, 870 (1984).
[28] P.C. Kelires, Phys. Rev. Lett. **68**, 1854 (1992).

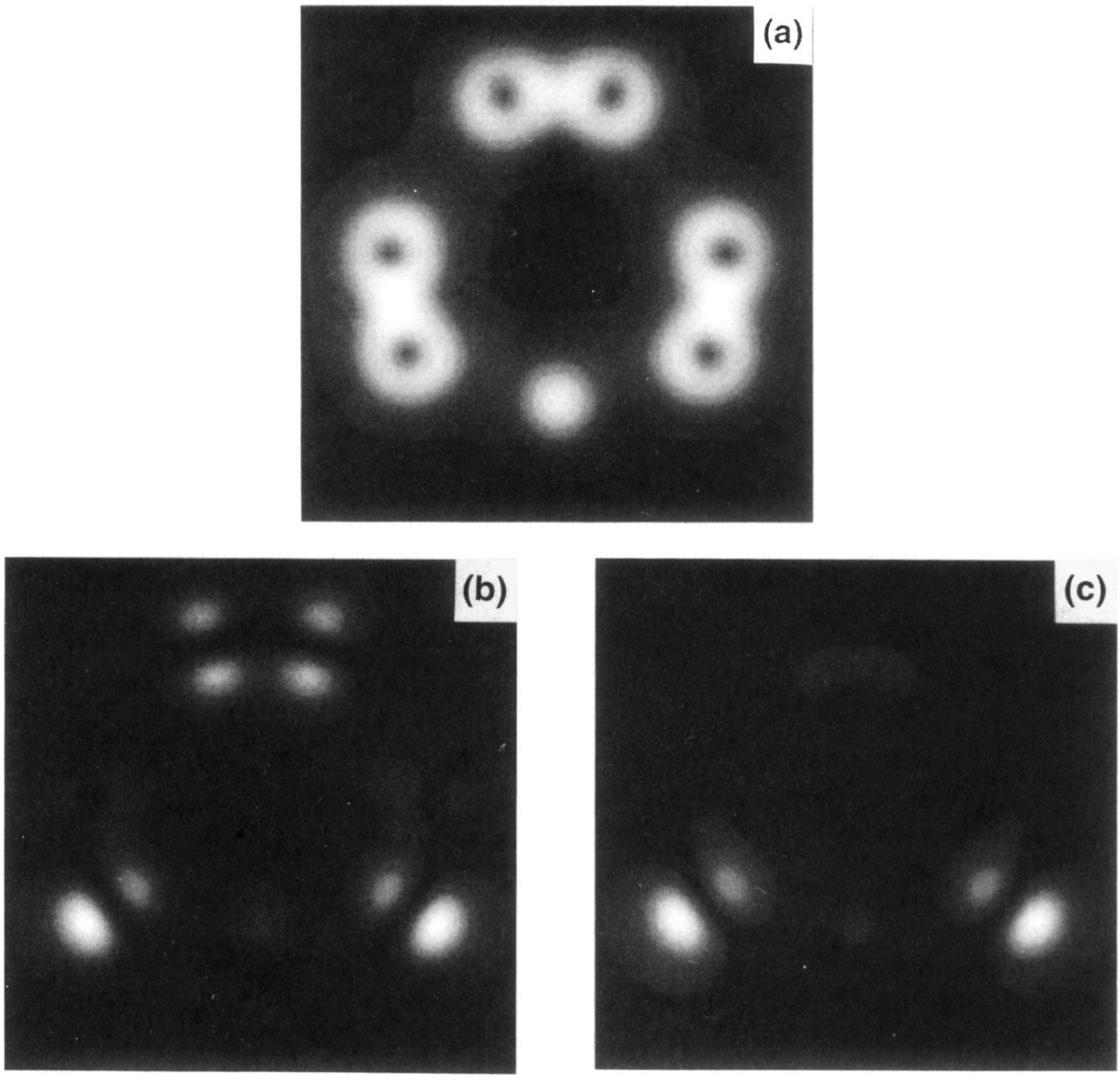

FIG. 3. (a) The total valence charge density on a cross section of the C_{28} cluster. The scale of electron density is represented by the brightness (the highest electron density is white). Each nearly vertical bond at the lower left and lower right hand sides of the figure is between one black atom and one white atom. Two different views of a bond between two white atoms that are not bonded to black atoms are shown at the top and bottom center of the figure. The upper bond is parallel to the plane of the figure and its entire length is shown, while the lower bond is perpendicular to the figure and a cross section at its midpoint is shown. Wave-function magnitude of the states near the Fermi level for (b) the triplet state t_2 (HOMO) and, (c) the singlet state a_1 (LUMO).

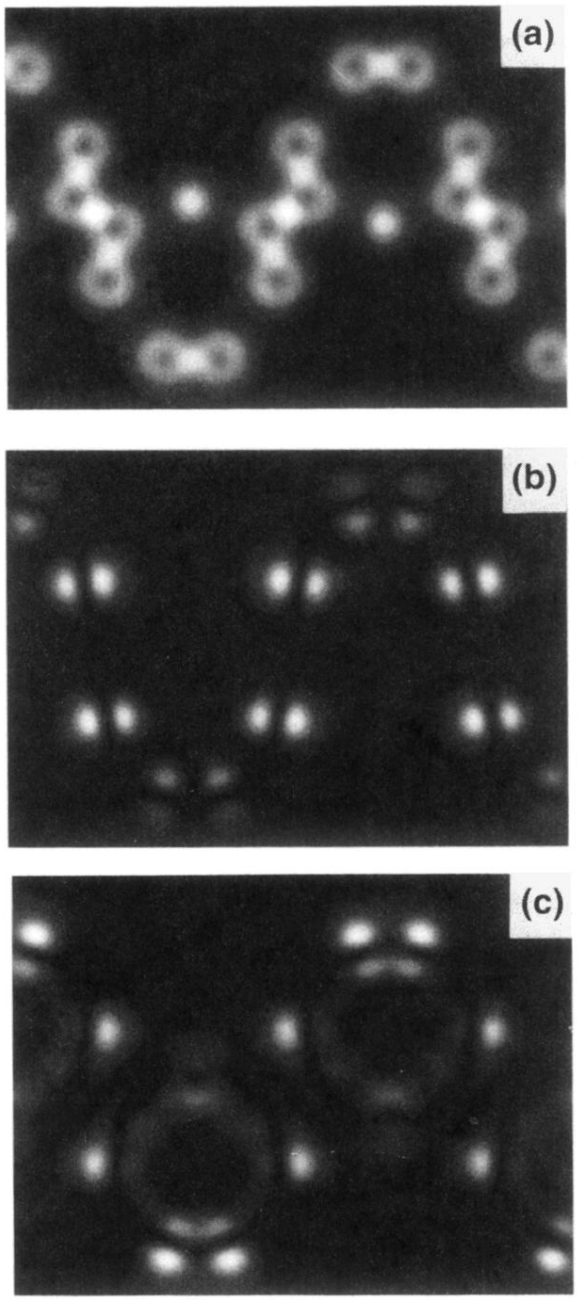

FIG. 4. (a) Valence charge density of hyperdiamond on the (110) plane. The only significant change from the charge density of an isolated C_{28} cluster is that intercluster bonds are formed at the tetrahedral apex atoms. Wave-function magnitude at Γ of hyperdiamond on the (110) plane for (b) the highest VBM state and (c) the lowest CBM state.